

# Lattice Boltzmann Simulation of Viscous Flow past Elliptical Cylinder

D. Arumuga Perumal<sup>1c</sup>, Gundavarapu V.S. Kumar<sup>2</sup> and Anoop K. Dass<sup>2</sup>

<sup>1</sup>Department of Aeronautical Engineering, Noorul Islam Centre for Higher Education, Noorul Islam University, Kanyakumari-629180, INDIA

<sup>2</sup> Department of Mechanical Engineering, Indian Institute of Technology Guwahati, Guwahati-781039, INDIA

Received: 14/05/2012 – Revised 13/08/2012 – Accepted 22/10/2012

## Abstract

This work is concerned with the vortex structures of two-dimensional elliptical cylinder by lattice Boltzmann method. It is known that, the nature of the flow past cylindrical obstacles is very complex. Therefore, in the present work a kinetic based approach, namely, lattice Boltzmann method is used to compute both for steady and unsteady flows. A two dimensional nine-velocity square lattice (*D2Q9*) model is used in the present simulation. Effects of blockage ratio, Reynolds number and channel length are studied in detail. Here we conclude that lattice Boltzmann method can be effectively used to capture vortex shedding and other features.

*Keywords: lattice Boltzmann method; D2Q9 model; viscous flow; elliptical cylinder; two-dimensional.*

## 1. Introduction

Over the years, the flow of fluids past cylinders of various cross sections has been a challenge and an interesting problem to researchers [1]. Bluff body flows constitute an important class of problems within the domain of fluid mechanics. The elliptical cylinder is also one of the important bluff objects referred in Computational Fluid Dynamics (CFD) field in which the aspect ratio and the angle of attack are the important parameters [2]. The present elliptical problem is one of the common analogues of many practical flow situations (e.g. tubular heat exchangers fitted with elliptical tubes, aerosol filters etc.). It is also known that, elliptical cylinders offer less flow resistance and higher heat transfer rates than circular cylinders.

Experimental and computational results of limited quantity are available for the flow past elliptical cylinder compared with other cylinders such as the circular and square cylinders confined in a channel [3-5]. In 1994, D'Alessio and Dennis [6] proposed a mathematical model for the steady two-dimensional flow of a viscous incompressible fluid past a cylinder. In 1996, Nair and Sengupta [7] have also investigated the flow field around circular and elliptic cylinders at zero angle of attack to study the onset of asymmetry in the near wake at high Reynolds numbers. In 2003, Dennis and Young [8] investigated the properties of steady two-dimensional flow past an elliptic cylinder

<sup>c</sup> Corresponding Author: D. Arumuga Perumal

Email: [d.perumal@iitg.ernet.in](mailto:d.perumal@iitg.ernet.in) Telephone: +91 361 2582654

© 2012 All rights reserved. ISSR Journals

Fax: +91 361 2690762

PII: S2180-1363(12)43127-X

inclined to the oncoming stream for small to moderate values of the Reynolds number. In 2010, Rao et al. [9] presented simulations of 2-D laminar flow of power-law fluids over elliptical cylinders with different aspect ratios.

In the last one and a half decade or so Lattice Boltzmann Method (LBM) has emerged as a new and effective approach of computational fluid dynamics and it has achieved considerable success in simulating fluid flows and heat transfer [10]. The LBM is based on constructing simplified kinetic models containing the physics of microscopic and mesoscopic processes so that averaging can recover macroscopic properties that obeys the continuum equations [11]. To demonstrate the ability of LBM, the present paper investigates the flow field characteristics of different Reynolds numbers for flow past an elliptical cylinder. The vortex shedding frequency depends on different aspects of the flow field such as the end conditions, blockage ratio of the flow passage. Another objective of this work is to investigate the influence of important parameters in the vortex shedding characteristics.

## 2. Lattice Boltzmann Method

### 2.1. Governing equation

The lattice Boltzmann method with single-relaxation-time (LBM-SRT) model with finite set of velocities is given by [12]

$$\frac{\partial f_a(\mathbf{x}, t)}{\partial t} + \xi_a \cdot \nabla f_a(\mathbf{x}, t) = -\frac{1}{\lambda} \left( f_a(\mathbf{x}, t) - f_a^{eq}(\mathbf{x}, t) \right) \quad (1)$$

where  $f_a(\mathbf{x}, t)$  and  $f_a^{eq}(\mathbf{x}, t)$  are the particle and equilibrium distribution functions associated with discrete velocity  $\xi_a$  at  $(\mathbf{x}, t)$  and  $\lambda$  is the relaxation time. It is known that, two-dimensional nine-velocity lattice model has been successfully used for simulating 2-D flows. The discretized form of governing equation can be written as [12]

$$f_i(\mathbf{x} + \mathbf{c}_i \Delta t, t + \Delta t) - f_i(\mathbf{x}, t) = -\frac{1}{\tau} \left[ f_i(\mathbf{x}, t) - f_i^{eq}(\mathbf{x}, t) \right] \quad (2)$$

where  $\mathbf{c}_i$  discrete velocity set and relaxation time  $\tau = \lambda / \Delta t$ . The  $D2Q9$  square lattice used here has nine discrete velocities. For the  $D2Q9$  model the discrete velocity set  $\{\mathbf{c}_i\}$  is written as [11]

$$\mathbf{c}_i = \begin{cases} (0, 0), & i = 0; \text{ group 0} \\ c(\pm 1, 0), c(0, \pm 1), & i = 1, 2, 3, 4; \text{ group I} \\ c(\pm 1, \pm 1), & i = 5, 6, 7, 8; \text{ group II} \end{cases} \quad (3)$$

In the above, group 0 indicates a rest particle, group I is for the links pointing to the nearest neighbors, group II is for the links pointing to the next-nearest neighbors.

The equilibrium distribution function for the  $D2Q9$  model is given by [10]

$$f_i^{(0)} = \rho w_i \left[ 1 - \frac{3}{2} \mathbf{u}^2 \right], \quad i = 0 \quad (4)$$

$$f_i^{(0)} = \rho w_i \left[ 1 + 3(\mathbf{c}_i \cdot \mathbf{u}) + 4.5 (\mathbf{c}_i \cdot \mathbf{u})^2 - 1.5 \mathbf{u}^2 \right], \quad i = 1, 2, 3, 4$$

$$f_i^{(0)} = \rho w_i \left[ 1 + 3(\mathbf{c}_i \cdot \mathbf{u}) + 4.5 (\mathbf{c}_i \cdot \mathbf{u})^2 - 1.5 \mathbf{u}^2 \right], \quad i = 5, 6, 7, 8$$

where  $w_i$  is the weighing factor given by

$$w_i = \begin{cases} 4/9, & i = 0; \\ 1/9, & i = 1, 2, 3, 4; \\ 1/36, & i = 5, 6, 7, 8. \end{cases} \quad (5)$$

With the discretized velocity space, the density and momentum fluxes can be evaluated as [12]

$$\rho = \sum_{i=0}^N f_i = \sum_{i=0}^N f_i^{eq} \quad (6)$$

$$\rho \mathbf{u} = \sum_{i=0}^N f_i \mathbf{c}_i = \sum_{i=0}^N f_i^{eq} \mathbf{c}_i \quad (7)$$

The speed of sound in this model  $c_s$  equals  $1/\sqrt{3}$  and the equation of state is that of an ideal gas [12]

$$p = \rho c_s^2 \quad (8)$$

The viscosity is related to the relaxation time by [11]

$$\nu = \left(\tau - \frac{1}{2}\right) c_s^2. \quad (9)$$

The density and the velocities satisfy the Navier-Stokes equations in the low-Mach number limit by using the Chapman-Enskog expansion [11].

## 2.2. Code Validation

First, the developed LBM code is used to compute the flow past a single circular cylinder confined in a channel. For a blockage ratio  $B = H/D = 8$  computations are carried out at  $Re = 60$  with the help of Lattice Boltzmann method (Diameter  $D = 10$ , Height  $H = 80$ ). The lattice size of  $500 \times 80$  is used for the configuration. In Table 1 we present the coefficient of drag for different steady-flow Reynolds numbers. Expectedly as the Reynolds number increases coefficient of drag ( $C_D$ ) decreases. It is worth mentioning that the numerical simulations of our LBM are much closer to existing available results.

TABLE 1: COEFFICIENT OF DRAG ( $C_D$ ) FOR DIFFERENT CIRCULAR CYLINDER STEADY-FLOW REYNOLDS NUMBERS BY LBM.

| Authors            | $Re=10$ | $Re=20$ | $Re=30$ | $Re=40$ |
|--------------------|---------|---------|---------|---------|
| Tritton [13]       | -       | 2.22    | -       | 1.48    |
| Fornberg [14]      | -       | 2.00    | -       | 1.50    |
| Calhoun [15]       | -       | 2.19    | -       | 1.62    |
| LBM – Present work | 3.21    | 2.25    | 1.74    | 1.50    |

## 2.3. Problem Description

In the present section, as shown in Figure 1, the flow configuration considered is similar to the circular cylinder except for the elliptical cross section of the cylinder. The present problem has a cylinder with elliptical cross section with minor axis  $D$  (major axis is parallel to the flow) that is mounted centrally inside a plane channel of height  $H$  with blockage ratio  $B = H/D = 16$ . The channel length  $L$  is fixed at  $L/D = 100$  to reduce the influence of outflow boundary conditions on accuracy. An upstream length of  $l = L/4$  (or  $25.0D$ ) has been chosen. In this problem, the inlet boundary conditions are given by a uniform velocity profile. The LBM simulation studies are carried out for different values of Reynolds numbers  $Re = \frac{UD}{\nu}$  where  $U$  is the velocity at the channel entry and  $D$  is the cylinder diameter.

## 2.4. Boundary Conditions:

In LBM, implementing the boundary condition is a difficult task because of the necessity of imposing conditions in terms of particle distribution functions. Boundary conditions on different walls are as follows:

Top and bottom walls: On the top and bottom walls, we use the well-known bounce-back boundary condition [10] which indicates no-slip. At the inlet boundary we impose bounce-back condition with momentum proposed by Yu et al. [12] can be written as

$$f_{\bar{i}}(\mathbf{x}_w, t + \Delta t) = f_{\bar{i}}(\mathbf{x}_w, t) + 2w_{\bar{i}}\rho \frac{3}{c^2} e_{\bar{i}} \cdot \mathbf{u}_w. \quad (10)$$

Outlet boundary: At the outlet boundary, we employ a second-order accurate extrapolation boundary condition, which is written as [16]

$$f_i(N_x, j) = 2 \times f_i(N_x - 1, j) - f_i(N_x - 2, j) \quad (11)$$

where  $N_x$  is the number of lattices in the  $x$ -direction. On the solid curved boundary, *i.e.*, on the surface of the cylinder, a robust second order accurate boundary treatment proposed by Bouzidi *et al.*, [17] is used for the particle distribution function.

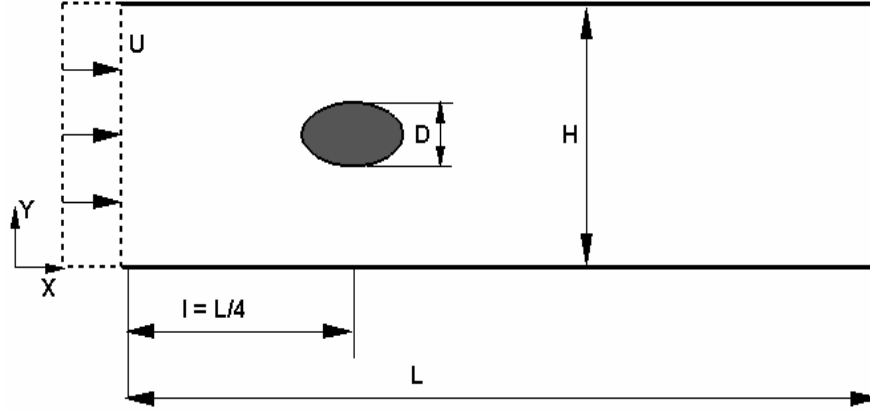


Figure 1. Schematic diagram of the flow past an elliptical cylinder confined in a channel.

### 2.5. Force Evaluation:

The momentum exchange method [12] is used for the force evaluation in the present work. The total resultant fluid force  $F$ , acting on a solid body by fluid can be written as [12]

$$F = \sum_{all x_b} \sum_{\alpha=1}^{N_d} e_{\bar{\alpha}} \left[ \tilde{f}_{\alpha}(x_b, t) + \tilde{f}_{\alpha}(x_b + e_{\bar{\alpha}} \delta t, t) \right] \times [1 - w(x_b + e_{\bar{\alpha}})] \delta x / \delta t \quad (12)$$

where  $N_d$  is the number of non zero lattice velocity vectors and  $w(x_b + e_{\bar{\alpha}})$  is an indicator, which is 0 at  $x_f$  and 1 at  $x_b$ . The two most important characteristic quantities of flow around a cylinder are the coefficient of drag and coefficient of lift. The coefficients are defined as [18]

$$\text{Coefficient of drag} \quad C_D = \frac{F_x}{\frac{1}{2} \times \rho U_a^2 D} \quad (13)$$

$$\text{Coefficient of lift} \quad C_L = \frac{F_y}{\frac{1}{2} \times \rho U_a^2 D} \quad (14)$$

where  $F_x$  and  $F_y$  are the  $x$  and  $y$  components of the total fluid force acting on the cylinder. In the present work, LBM computations for steady state are carried out till the following convergence criterion is satisfied

$$\frac{\sqrt{\sum_{i,j} [\mathbf{u}_{i,j}^{k+1} - \mathbf{u}_{i,j}^k]^2}}{\sqrt{\sum_{i,j} [\mathbf{u}_{i,j}^{k+1}]^2}} \leq 1 \times 10^{-6} \quad (15)$$

where  $u_{i,j}$  is the fluid velocity and  $k$  is the iteration level.

#### Themes of Studies are as follows:

- (i) For a fixed blockage ratio to study the elliptical cylinder flow field characteristics for various Reynolds numbers.
- (ii) For different blockage ratios to study the elliptical cylinder flow field characteristics.
- (iii) For different lengthwise cylinder locations to study the flow field characteristics.
- (iv) For different outlet boundary locations to study the elliptical cylinder flow field characteristics.

### 3. Results and discussion

#### *Case (i): Fixed Blockage Ratio*

For a blockage ratio  $B = H/D = 16$  computations are carried out at different Reynolds numbers with the help of Lattice Boltzmann method with single-relaxation-time collision model. The lattice size of  $800 \times 128$  is used for the present configuration.

#### *Steady flow:*

Streamline patterns for a blockage ratio of 16 at Reynolds numbers  $Re = 3, 30, 50$  and  $60$  is shown in Figure 2. At low Reynolds number ( $Re = 3$ ) the steady flow past the elliptical cylinder persists without separation as shown in Figure 2(a). As Reynolds number increases the separation of the steady flow laminar boundary layer is clearly observed in Figure 2(b) - 2(d). It is seen (Figure 2(b) - 2(d)) that two vortices downstream of the cylinder, symmetrically placed about the channel centreline, develop and remain attached to the cylinder. From figures 2(b) - 2(d), it is again seen that for steady flows the size of the vortices increases with Reynolds number.

#### *Unsteady flow:*

In our LBM simulation the periodic flow is computed at  $Re = 100$  and  $150$  for which the streamline patterns at a certain instant are shown in Figures 3(a) and 3(b). From the Figures 3(a) and 3(b) it is seen that, as the Reynolds number increases beyond a certain critical value the streamline patterns becomes wavy and sinuous on the rear-side of the elliptical cylinder.

Figure 4 depicts the vorticity contours for flow past an elliptical cylinder at different Reynolds numbers ( $Re = 3, 30, 60, 100$  and  $150$ ). Interestingly for the steady flow, on the line of symmetry downstream of the cylinder flow is irrotational. Steady flow vortices seem to be more and more elongated as the Reynolds number increases. From the vorticity contours we clearly observe that vortices with negative and positive vortices are alternatively shed at  $Re = 100$  and  $150$ . This is known as the famous von Karmann vortex street. The point of separation is also clearly observed from the vorticity contours.

From Figures 4(d) and 4(e) it is seen that for a fixed length of the confining channel number of periodic vortices shed increases with Reynolds number. Thus without quantifying the associated frequencies for the Reynolds numbers, it is possible to say that frequency of vortex shedding increases as Reynolds number increases. The pressure contours for the flow past an elliptical

cylinder at different Reynolds numbers are shown in Figure 5. It is observed that from Figure 5(b) in the wake region the alternative vortices are clearly visible for  $Re=100$ .

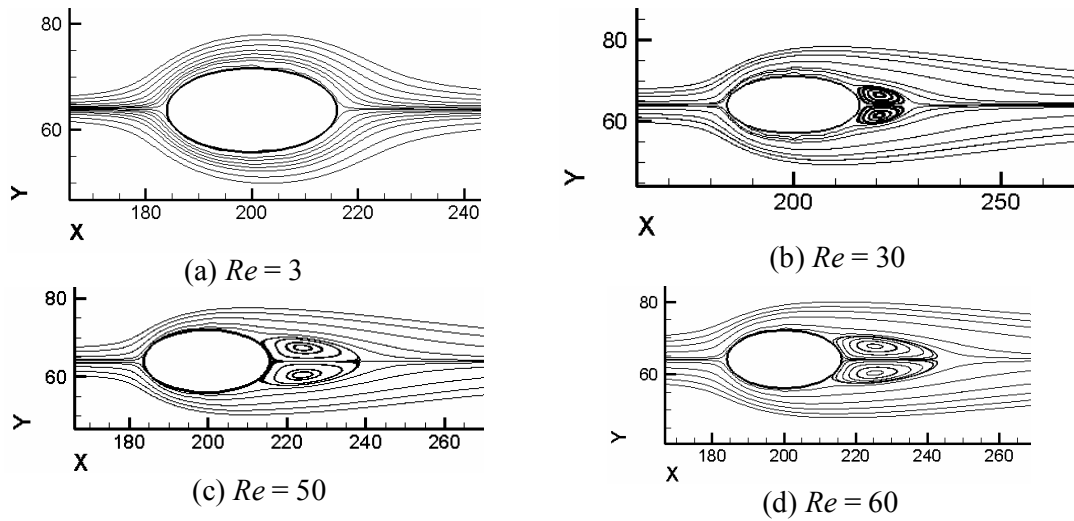


Figure 2. Streamline patterns for steady flows past an elliptical cylinder at different Reynolds numbers for a blockage ratio ( $B$ ) of 16: (a)  $Re=3$  (b)  $Re=30$  (c)  $Re=50$  (d)  $Re=60$ ; Lattice size:  $800 \times 128$ .

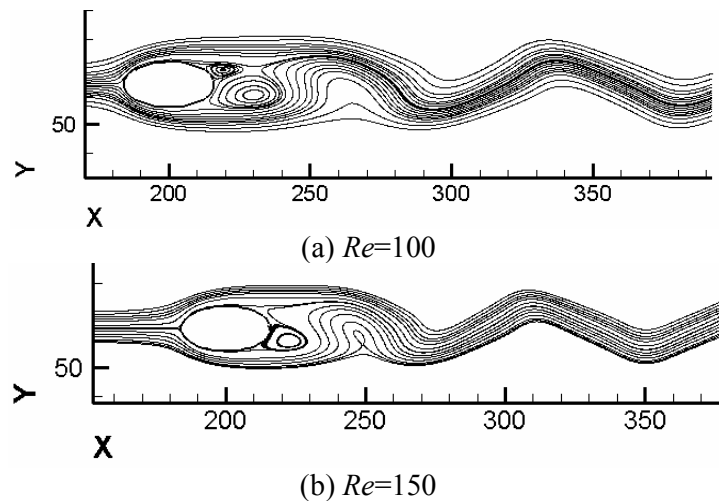


Figure 3. Instantaneous streamline patterns for flows past an elliptical cylinder at different Reynolds numbers for a blockage ratio ( $B$ ) of 16: (a)  $Re=100$  (b)  $Re=150$ ; Lattice size:  $800 \times 128$ .

In order to study the flow field characteristics, velocity variation along the channel centerline are presented for  $Re = 150$ . Figure 6 shows the distribution of  $x$ - and  $y$ - velocity components along the channel centreline. It is observed that fluctuations of velocity at the exit boundary are small. At the surface of the cylinder velocity is zero and at upstream locations flow velocity varies smoothly without much oscillation. Figure 7 shows velocity profiles of  $u$  and  $v$  at three different axial positions,  $x = 192, 292$  and  $492$ . From the figures we can clearly observe that velocity profiles, typical of the wake region, do not exhibit any orderly trend.

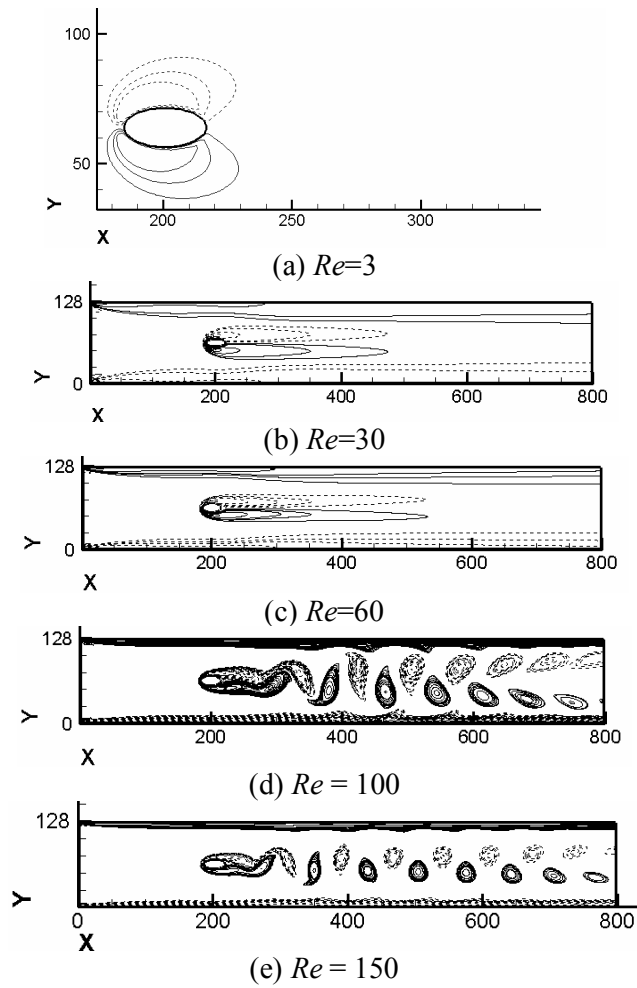


Figure 4. Vorticity contours around the elliptical cylinder for different Reynolds numbers with  $B=16$ . (a)  $Re=3$ ; (b)  $Re=30$ ; (c)  $Re=60$ ; (d)  $Re=100$  and (e)  $Re=150$ ; Lattice size :  $800 \times 128$ .

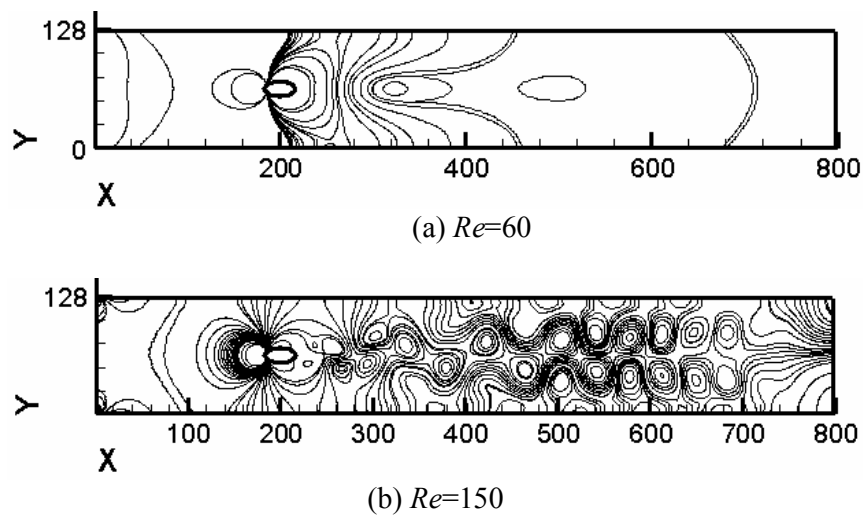


Figure 5. Instantaneous pressure contours around the elliptical cylinder for different Reynolds numbers with  $B=16$ . (a)  $Re=60$ ; (b)  $Re=100$ ; Lattice size :  $800 \times 128$ .

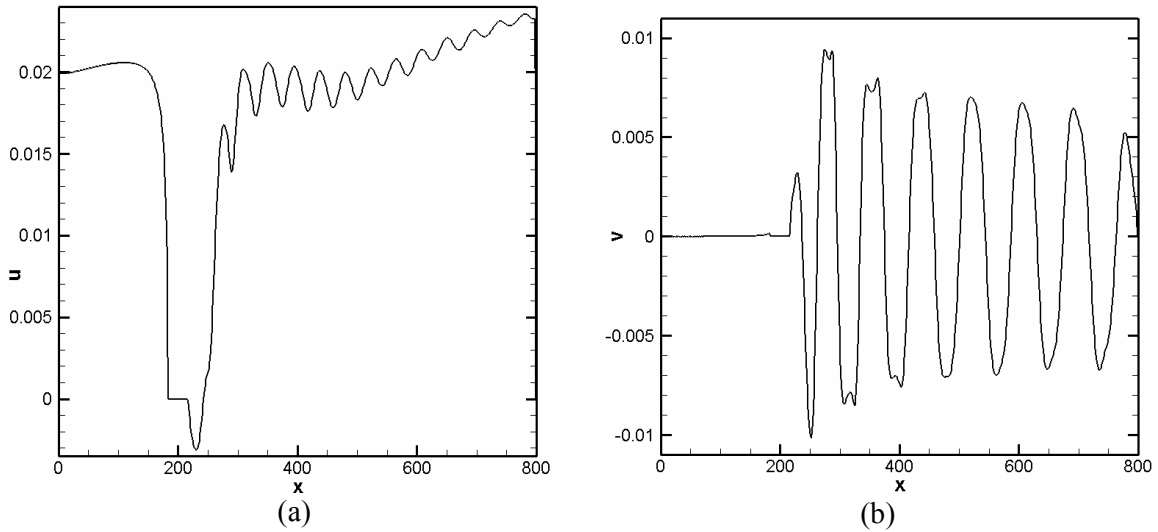


Figure 6. Instantaneous results at a certain moment for the flow over an elliptical cylinder: (a) streamwise ( $u$ ) and (b) cross-stream ( $v$ ) velocities long the centerline ( $y=64$ );  $Re=150$ , Lattice size:  $800 \times 128$ .

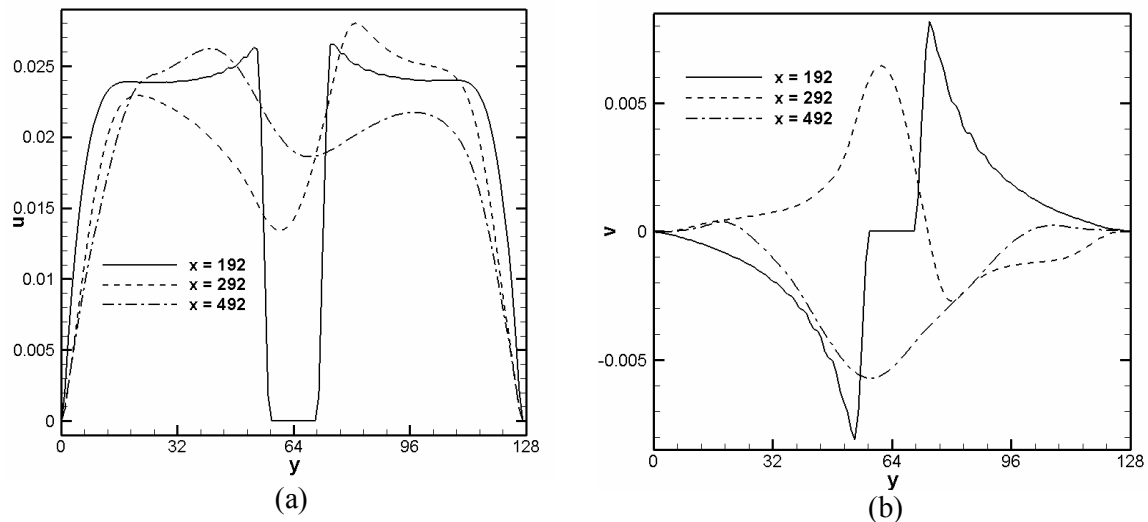


Figure 7. Instantaneous results at a certain moment for the flow over an elliptical cylinder: (a) streamwise ( $u$ ) and (b) cross-stream ( $v$ ) velocities at three different positions in the flow field, center of cylinder ( $x=192$ ), near-wake ( $x=292$ ) and far-wake ( $x=492$ ) at  $Re=150$  and Lattice size of  $800 \times 128$ .

Figure 8 depicts the instantaneous streamline pattern and vorticity contours for  $Re = 78$ . It is seen that from the present LBM computations unsteadiness develops for this Reynolds number and it leads to periodic vortex shedding without any triggering.

Figure 9 shows the periodic time variation of the lift coefficient ( $C_L$ ) and drag coefficient ( $C_D$ ) for the flow past an elliptical cylinder at  $Re = 100$  and  $150$ . It is seen that for each time period,  $C_D$  has two crests and two troughs of unequal amplitudes, which are a consequence of the periodic vortex shedding from the top and bottom surfaces. The same figure shows that  $C_L$  for each time period has just one trough and one crest; this is because  $C_L$  is not influenced by the pressure distribution on the rear side of the cylinder, which is strongly influenced by the vortex shedding at the top and bottom sides of the cylinder. The value of the lift force fluctuation is directly connected

to the formation and shedding of the eddy and, therefore, its value varies between a positive maximum and a negative maximum of equal magnitude. In Table 2, we present the mean drag coefficient for different Reynolds numbers. It is seen that as Reynolds number increases coefficient of drag decreases.

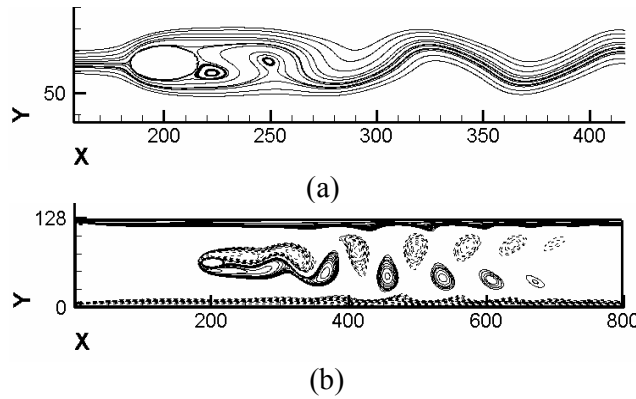


Figure 8. Instantaneous streamline pattern and vorticity contours for flows past an elliptical cylinder at  $Re = 78$ ,  $B = 16$ ; Lattice size :  $800 \times 128$ .

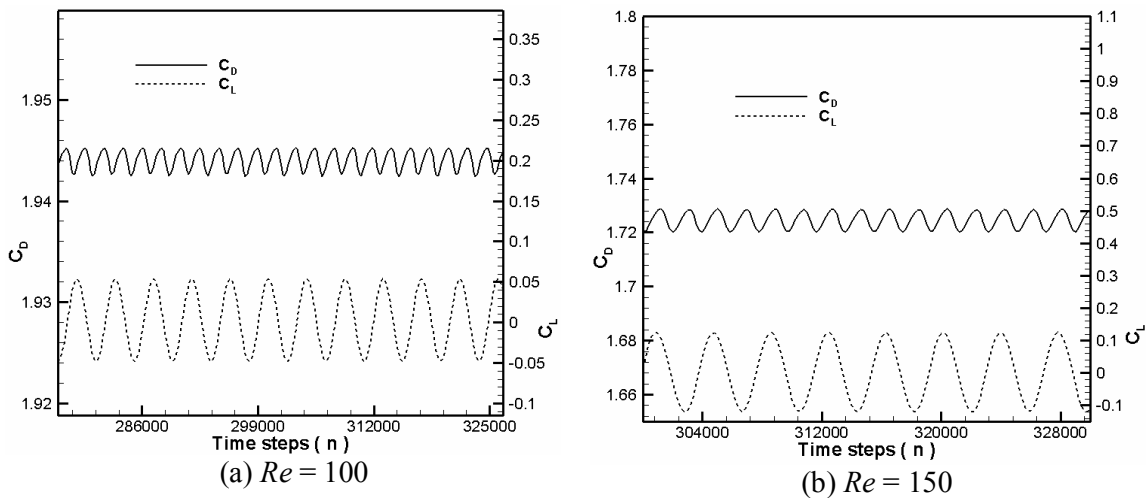


Figure 9. Flow past an elliptical cylinder: Time-dependent lift and drag coefficients ( $C_L$  and  $C_D$ ) at (a)  $Re=100$  and (b)  $Re=150$  on a lattice size of  $800 \times 128$ .

TABLE 2: MEAN DRAG COEFFICIENT FOR THE FLOW OVER AN ELLIPTICAL CYLINDER AT DIFFERENT REYNOLDS NUMBERS.

| Authors            | $Re=100$ | $Re=150$ |
|--------------------|----------|----------|
| LBM – Present Work | 1.942    | 1.725    |

**Case (ii): Different blockage ratios**

The change in blockage ratio ( $B$ ) has been accomplished just by changing the channel height ( $H$ ). In order to study the effect of different blockage ratios  $Re = 78$  is chosen in the present work. Cylinder location of  $l = L/4$  and a channel length of  $L/D = 100$  is considered here. Figure 10 shows the instantaneous vorticity contours for confined flow over an elliptical cylinder at different

blockage ratios. Four different blockage ratios  $B = 8, 10, 16$  and  $20$  are studied in the present work. From our LBM simulations we observed that the moderate blockage ratio  $B = 16$  onwards unsteadiness develops in the flow field. The flow appears to be steady in the lower blockage ratios. As the blockage ratio increases computation time required for developing unsteadiness increases. It can be clearly observed from figure 10 that at low blockage ratios wall boundary layer has strong influence over around the cylinder so that it inhibits vortex shedding.

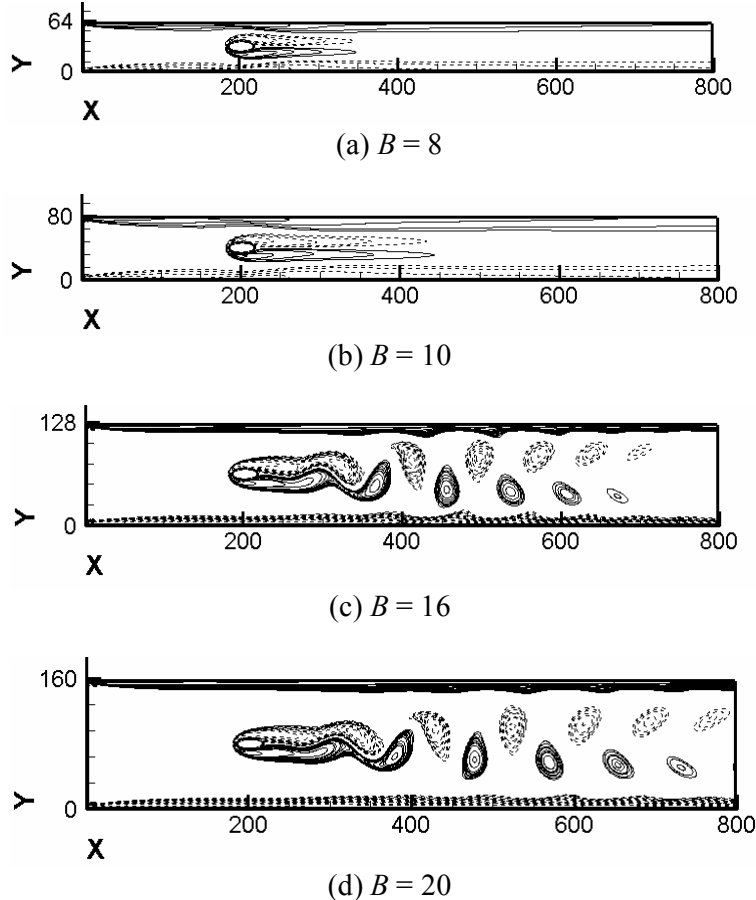


Figure 10. Instantaneous vorticity contours for flows past an elliptical cylinder at different blockage ratios (a)  $B = 8$  (b)  $B = 10$  (c)  $B = 16$  and (d)  $B = 20$ .

### ***Case (iii): Different cylinder locations***

To study the effect of different cylinder locations  $Re = 78$  is chosen in the present work. In this section, blockage ratio  $B = 16$  and  $L/D = 100$  is considered. All the cases studied so far take  $l = 12.5D$ . In the present case,  $l = 50.0D, 25.0D, 20.0D$  and  $10.0D$  is considered. Figure 11 shows the instantaneous vorticity contours for confined flow over an elliptical cylinder at different cylinder locations. It is seen that only for the cylinder location of  $25.0D$  and beyond the vortex shedding appears. Also differences in the size and strength of the vortices are observed as the cylinder location changes. This can be attributed to the fact that at different cylinder locations the wall boundary layer produces different affects. Also as  $l$  increases, the exit boundary may come too near for the prescribed outflow boundary condition to hold accurately. The frequency of vortex shedding increases as the location of the cylinder moves upstream.

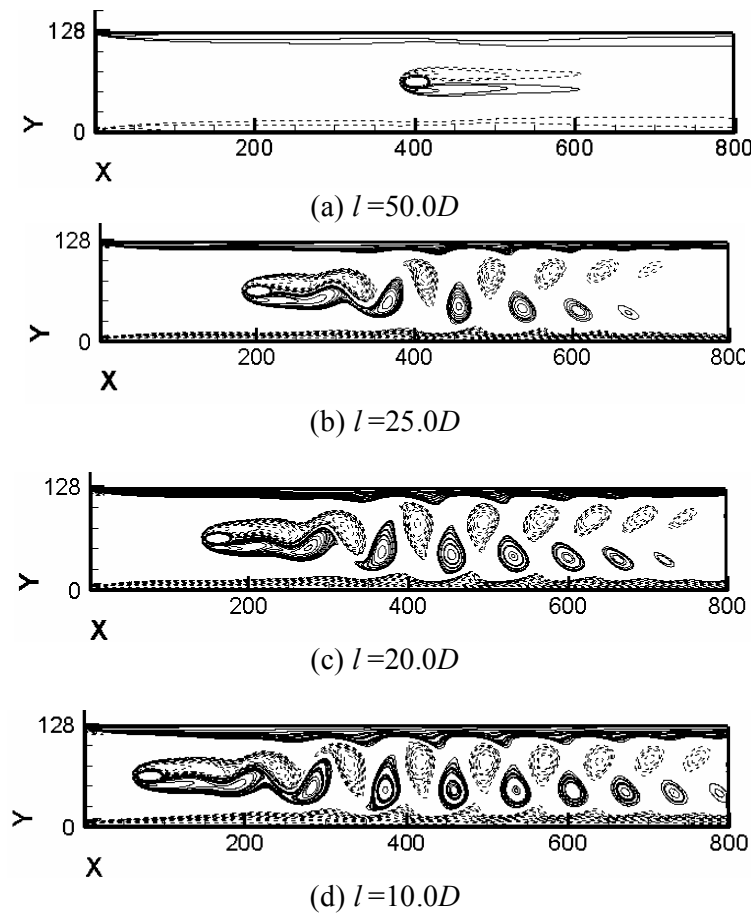


Figure 11. Instantaneous vorticity contours for simulation of flow past an elliptical cylinder at  $Re=78$  for different cylinder locations: (a)  $l=50.0D$ ; (b)  $l=25.0D$ ; (c)  $l=20.0D$ ; (d)  $l=10.0D$ : Lattice size of  $800 \times 128$ .

#### **Case (iv): Different outlet boundary locations**

To study the effect of different outlet boundary locations  $Re = 78$  is taken. In this case, blockage ratio  $B = 16$  and upstream length  $l = L/4$  is chosen. Here  $L/D = 40, 50, 80$  and  $100$  are considered. Figure 12 shows the instantaneous vorticity contours for confined flow over an elliptical cylinder at different outlet boundary locations. It is clearly observed that the outlet boundary location is also playing important role in the vortex shedding process for a particular Reynolds number. For the extrapolation boundary condition for the particle distribution function at the outlet boundary to hold accurately, the boundary should be far enough downstream of the cylinder. In our present study, simulation results reveal the fact that  $L/D = 50$  onwards periodic solutions are obtained for the  $Re = 78$ .

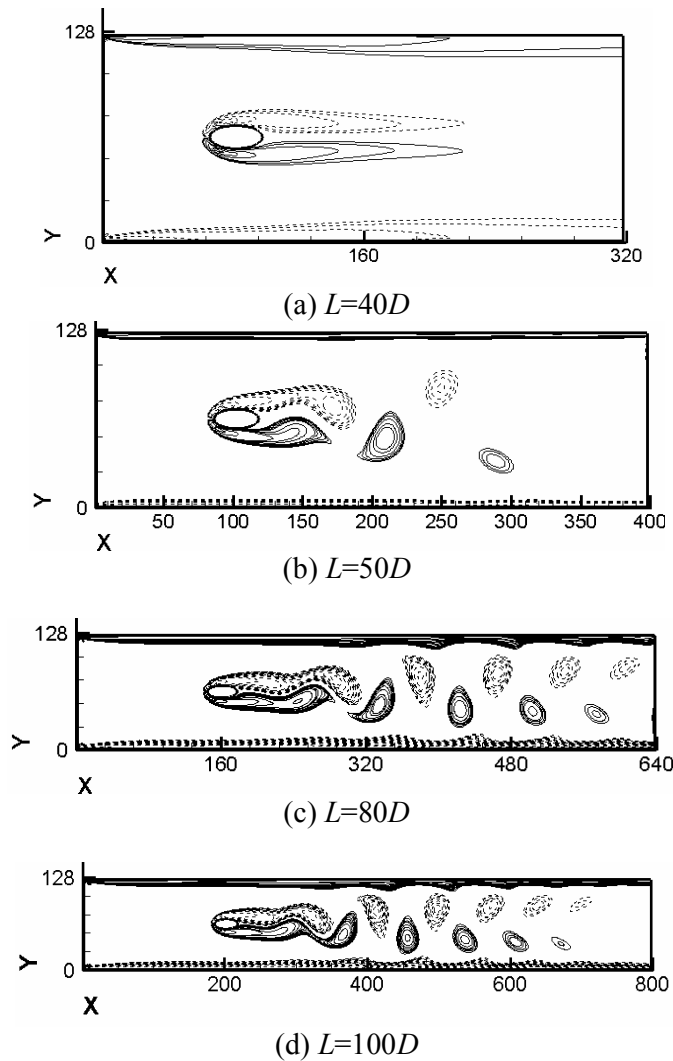


Figure 12. Instantaneous vorticity contours for simulation of flow past an elliptical cylinder at  $Re=78$  for different outlet boundary locations: (a)  $L=40D$ ; (b)  $L=50D$ ; (c)  $L=80D$  and (d)  $L=100D$ .

#### 4. Conclusion

In the present work, to understand the flow past the elliptical cylinder we examine four different cases. First, we investigate the elliptical cylinder flow field characteristics at different Reynolds numbers. For a blockage ratio ( $B = 16$ ) we found that periodicity starts at  $Re = 78$ . Next, we examine different blockage ratios at  $Re = 78$ . We conclude that as the blockage ratio increases the frequency of the vortex shedding increases. Then, we study different upstream locations at  $Re = 78$ . We observe that as cylinder is located nearer to the entrance the periodicity develops faster. It is worth mentioning that the similar trend is also observed in the square cylinder problem. Next, we investigate different outlet boundary locations. It is seen that, as the length of the portion of the channel downstream increases the flow gets periodic behaviour faster. It is concluded that, we examine different cases and the present Lattice Boltzmann Method computations bring out many interesting features. The present work can be extended to three-dimensional computations and higher Reynolds numbers for different cylinders. Another interesting extension is to study the flow past a triangular cylinder confined in a channel.

## References

- [1] Mittal, R., and S. Balachandar, *Direct Numerical Simulation of flow past elliptic cylinders*, Journal of Computational Physics, 1996. **124**: p. 351-367.
- [2] Shintani, K., A. Umemura and A. Takano, *Low-Reynolds-number flow past an elliptic cylinder*, Journal of Fluid Mechanics, 1983. **136**: p. 277-289.
- [3] Khan, W.A., J.R. Culham, and M.M. Yovanovich, *Fluid Flow Around and Heat Transfer from Elliptical Cylinders: Analytical Approach*, Journal of Thermodynamics and Heat Transfer, 2001. **19**: p. 178-185.
- [4] Heidarinejad, G. and Delfani, S, *Simulation of Wake Flow Behind an Elliptical Cylinder at High Reynolds Number by Random Vortex Method*, 6th Fluid Dynamic Conference, Iran University of Science and Technology, Tehran, Iran, (In Farsi), (1999), p. 199-210.
- [5] Jackson C.P., *A finite-element study of the onset of vortex shedding in flow past variously shaped bodies*, Journal of Fluid Mechanics, 1987. **182**: p. 23-45.
- [6] D'alessio, S. J. D. and S. C. R. Dennis, *A Vorticity model for viscous flow past a cylinder*, Computers & Fluids, 1994. **23**: p. 279-293.
- [7] Nair, M. T. and T. K. Sengupta, *Unsteady flow past elliptic cylinders*, Journal of Fluids and Structures, 1997. **11**: p. 555 – 595.
- [8] Dennis S.C.R. and P.J.S. Young, *Steady flow past an elliptic cylinder inclined to the stream*, Journal of Engineering Mathematics, 2003. **47**: p. 101–120.
- [9] Rao, P.K., A.K. Sahu, and R.P. Chhabra., *Flow of Newtonian and Power-Law Fluids Past an Elliptical Cylinder: A Numerical Study*, Ind. Eng. Chem. Res. 2010. **49**: p. 6649-6661.
- [10] Perumal, D.A., and A.K. Dass, *Simulation of Incompressible Flows in Two-Sided Lid-Driven Square Cavities, Part II-LBM*, CFD Letters, 2010. **2** (1): p. 25-38.
- [11] Perumal, D.A., and A.K. Dass., *Multiplicity of steady solutions in two-dimensional lid-driven cavity flows by the Lattice Boltzmann method*, Computers & Mathematics with Applications, 2011. **61**: p. 3711-3721.
- [12] Yu, D., R. Mei, and L.S. Luo, *Viscous flow computations with the method of Lattice Boltzmann equation*, Progress in Aerospace Sciences, 2003. **39**: p. 329-367.
- [13] Tritton, D.J., *Experiments on the flow past a circular cylinder at low Reynolds numbers*, Journal of Fluid Mechanics, 1959. **6**: p. 547-555.
- [14] Fornberg, B., *A numerical study of steady viscous flow past a circular cylinder*, Journal of Fluid Mechanics, 1980. **98**: p. 819-855.
- [15] Calhoun., D., *A cartesian grid method for solving the two-dimensional streamfunction-vorticity equations in irregular regions*, Journal of Computational Physics, 2002, **176**: p. 231–275.
- [16] Guo, Z., C. Zheng, and B. Shi, *An extrapolation method for boundary conditions in lattice Boltzmann method*, Physics of Fluids, 2002. **14**: p. 2007-2010.
- [17] Bouzidi, M., M. Firdaouss, and P. Lallamand, *Momentum transfer of a lattice Boltzmann fluid with boundaries*, Physics of Fluids, 2001. **13**: p. 3452-3459.
- [18] Kumar, G.V.S., D.A. Perumal, and A.K. Dass, *Numerical simulation of viscous flow over a circular cylinder using Lattice Boltzmann method*, in: *Proceedings of the International Conference on Fluid Mechanics and Fluid Power*, FMFP 2010, Dec 16-18, Indian Institute of Technology Madras, India.
- [19] Bharti R.P, Sivakumar, P, Chhabra, R.P, *Forced convection heat transfer from an elliptical cylinder to power-law fluids*, International Journal of Heat and Mass Transfer, 2008. **51**: p. 1838-1853.
- [20] Wang J, Pui, D.Y.H., *Filtration of aerosol particles by elliptical fibers: A numerical study*, Journal of Nanoparticle Research, 2009. **11**: p. 185-196.